2006-03-16

Membrane-Based Protein Preconcentration Microfluidic Devices

Yi Li
Brigham Young University - Provo

MEMBRANE-BASED PROTEIN PRECONCENTRATION MICROFLUIDIC DEVICES

by

YI LI

A thesis submitted to the faculty of

Brigham Young University

in partial fulfillment of the requirements for the degree of

MASTER OF SCIENCE

Department of Chemistry and Biochemistry

Brigham Young University

April 2006

BRIGHAM YOUNG UNIVERSITY

GRADUATE COMMITTEE APPROVAL

of a thesis submitted by

Yi Li

This thesis has been read by each member of the following graduate committee and by majority vote has been found to be satisfactory.

Date	Adam T. Woolley, Chair
Date	Milton L. Lee
Date	Paul B. Farnsworth
Date	Dennis Tolley

BRIGHAM YOUNG UNIVERSITY

As chair of the candidate's graduate committee, I have read the thesis of Yi Li in its final form and have found that (1) its format, citations, and bibliographical style are consistent and acceptable and fulfill university and department style requirements; (2) its illustrative materials including figures, and charts are in place; and (3) the final manuscript is satisfactory to the graduate committee and is ready for submission to the university library.

Date

Adam T. Woolley
Chair, Graduate Committee

Accepted for the Department

David V. Dearden
Graduate Coordinator

Accepted for the College

Tom Sederberg
Associate Dean, College of Physical
and Mathematical Sciences

ABSTRACT

MEMBRANE–BASED PROTEIN PRECONCENTRATION MICROFLUIDIC DEVICES

Yi Li

Department of Chemistry and Biochemistry

MASTER OF SCIENCE

Interest in microchip capillary electrophoresis (CE) is growing due to the rapid analysis times provided and small sample input requirements. However, higher-concentration samples are typically needed because of the small (~pL) detection volumes in these devices. I have made membrane-based protein preconcentration systems in capillary and microchip designs to increase the detectability of low-concentration biological samples. A photopolymerized ion-permeable membrane interfaced with a microchannel in poly(methyl methacrylate) (PMMA) formed the preconcentrator. When a voltage was applied between the sample reservoir and the ionically conductive membrane in a capillary-based system, R-phycoerythrin was concentrated more than 1,000

fold, as determined by laser-induced fluorescence measurement. An integrated system that combines analyte preconcentration with microchip CE has also been developed using two different fabrication methods: polymerization and solvent bonding. In both approaches, microchannels within the PMMA substrates were interfaced with an ion-permeable hydrogel. When an electrical potential was applied along the channel, greater than 10,000-fold preconcentration was achieved for R-phycoerythrin. Concentrated protein samples were also injected and separated in these integrated microdevices. Membrane-based protein preconcentration devices can significantly increase the concentration range of biological samples that can be analyzed by microchip CE.

ACKNOWLEDGEMENTS

First of all, I thank my advisor, Dr. Adam T. Woolley, for giving me the chance to finish this interesting project, providing very useful advice, and his great patience with me. I also thank my graduate committee members, Dr. Milton L. Lee, Dr. Paul B. Farnsworth and Dr. Dennis Tolley for their valuable suggestions and help. I give Dr. Ryan T. Kelly special thanks for his instrumentation training, very helpful ideas, and very kind patience. I thank Dr. Paul Humble for developing the ion-permeable copolymer, which was necessary for both the capillary-based microdevices and the integrated microchip systems. I also thank Xuefei Sun, Tao Pan, Jikun Liu, and Bridget Peeni for their great help in my project. My lab mates and other friends in the department have been helpful and have made the experience enjoyable. I am grateful to the National Institutes of Health for research funding. Finally, I thank the BYU Integrated Microelectronics Laboratory, the Department of Chemistry and Biochemistry, and Brigham Young University.

TABLE OF CONTENTS

Page

LIST OF FIGURES

1. INTRODUCTION

1.1 Analytical Separation

A separation is a process by which a mixture of chemical components is resolved, ideally into individual constituents. In chemical analysis, separations are used as a tool to provide qualitative and quantitative information about the chemical composition of complex mixtures. In analytical separations, the mixed compounds are differentially transported through a distance until they are separated into fractions that are distinguishable from one another. Separation technology plays a very important role in analytical chemistry and has become an indispensable step in numerous industrial processes.

Separation methods have been key in the characterization of biologically important proteins and peptides, as illustrated by the following examples. An integrated concentration and separation platform that interfaces capillary isoelectric focusing with capillary reversed-phase liquid chromatography has been shown to enrich proteins ~240 fold [1]. Reversed-phase high performance liquid chromatography with a saw-tooth gradient has been reported for the separation of human serum [2]. A multiple gel system has been applied in the analysis of the proteome of human pituitary tissue, and over 1,000 individual proteins were separated [3]. Finally, immobilized metal affinity chromatography has been developed to separate homologous human blood proteins based on their

metal-binding properties [4]. These examples demonstrate the growing importance of separation science in protein characterization.

Separation methods can be classified by the mechanism of analyte transport through the column. Pressure-driven techniques include the majority of column chromatographies that are based on partitioning, adsorption, and the interaction between solutes, mobile phase, and stationary phase. Liquid chromatography, gas chromatography and supercritical fluid chromatography are all pressure-driven approaches. On the other hand, electrically driven methods are based on the differential migration of charged species via electrophoretic and electroosmotic effects in an electric field. Slab gel electrophoresis and capillary electrophoresis (CE) are examples of electrically driven methods. In my thesis, I will focus mainly on separation by electrical means such as CE.

1.2 Capillary Electrophoresis

Capillary electrophoresis is a separation technique that employs 20-100 μm internal diameter (ID) fused silica capillaries that are filled with a conductive liquid under an electric field. In CE, samples are placed at the start of a buffer-filled column, and then a high voltage (10-30 kV) is applied between the ends of the capillary to serve as the driving force for charged sample molecules. Negatively charged analytes migrate toward the electrode with positive polarity, and positively charged species

move toward the electrode with negative polarity. Fractionation occurs based on charge and analyte size; CE can separate both large molecules such as proteins and small ions. CE was developed by Verheggen's group at Eindhoven [5] and Jorgenson's group at the University of North Carolina [6]. Verheggen's group showed high-performance capillary zone electrophoresis (CZE) in 0.2 mm ID narrow-bore tubes for separating a 16-component sample [5]. Jorgenson and Lukacs used 75 μm ID, 80-100 cm long glass open tubular capillaries with 30 kV applied to separate amino acids, peptides, and urinary amines [6]. Since these initial studies, the field of CE has expanded tremendously and a variety of electrically driven methods have been developed, including CZE, capillary gel electrophoresis (CGE), micellar electrokinetic capillary chromatography (MEKC) and others.

The speed with which a charged species travels in electrophoresis is determined by the applied electric field, the electrophoretic mobility of the species and the electroosmotic mobility.

$$v = (\mu_{ep} + \mu_{eo})E = (\mu_{ep} + \mu_{eo})V / L \tag{1.1}$$

In (1.1), v is the migration velocity, E is the electric field, μ_{ep} is the electrophoretic mobility, μ_{eo} is the electroosmotic mobility, V is the applied potential and L is the separation distance or column length. Because E and μ_{eo} are the same for all species present in a mixture, different analytes can be separated according to just μ_{ep}. Electrophoretic mobility is given by

$$\mu_{ep} = q / 6r\pi\eta \quad (1.2)$$

where q is the net charge of the species, r is the Stokes' radius and η is the buffer viscosity. The efficiency of a separation is expressed in terms of the number of theoretical plates (N) [7],

$$N=V(\mu_{eo}+\mu_{ep})/2D \quad (1.3)$$

where D is the diffusion coefficient. From (1.3) it is evident that separation efficiency increases with the applied potential and is independent of the dimensions of the capillary.

In CZE, samples are introduced into one end of a capillary that is filled with a conductive solution, and since (1.3) indicates that N scales with V, high voltage (10-30 kV) is applied along the column. In the applied potential, solutes migrate through the capillary according to μ_{ep}, which depends on the charge-to-size ratio, as shown in (1.2). Thus, during a run, different analytes are separated into discrete zones according to μ_{ep}. For optical detection, a transparent window near the end of the capillary is used to detect the separated analytes.

The surface of fused silica capillaries has negatively charged silanol (Si-OH) groups that cause a layer of cations to build up near the surface to maintain charge balance. This creates a double layer of ions near the surface and a potential difference called the zeta potential. When a voltage is applied along the length of such a capillary, the cations forming the double layer are attracted to the cathode and drag

the bulk solution through the capillary toward the cathode. This phenomenon is referred to as electroosmotic flow (EOF). The magnitude of EOF scales with the density of charged groups on the surface of the capillary. In addition, EOF is strongly dependent on the pH of the buffer solution, since the zeta potential is determined by the surface charge density on the capillary wall, which is pH dependent. Several methods are used to control EOF in CE, including adjustment of buffer pH or concentration, controlling capillary temperature, covalently coating the capillary walls or adding a neutral hydrophilic polymer [8].

CGE is a similar technique to CZE, because both are electrically driven separation methods and fractionate molecules by mobility. However, in CGE the capillary is filled with a porous gel or sieving matrix such as polyacrylamide, unlike in CZE [9]. When charged molecules are introduced into a gel-filled capillary, they are fractionated based on their size by a sieving mechanism. Smaller molecules move more quickly through the pores of the gel and elute faster, while larger molecules must undergo conformational changes to traverse the pores and elute slower. CGE is used in separations of DNA, proteins and other macromolecules.

CZE and CGE have been applied in the analysis of proteins and peptides [9, 10]. Peptides are usually well separated using CZE [11]; however, the separation of proteins by CZE is often unsatisfactory because proteins are usually larger and have more complicated structures than peptides. CGE or multidimensional separation

methods perform separation of proteins well. Other techniques can also be chosen to separate proteins, including isoelectric focusing and MEKC [9].

1.3 Improving Capillary Electrophoresis

One aim of CE is to rapidly and accurately analyze biological samples. The analysis time t is [7]

$$t=L^2/V(\mu_{eo}+\mu_{ep}) \tag{1.4}$$

Thus, the analysis time can be reduced considerably by shortening the separation column or increasing the applied potential. In addition, (1.3) indicates that separation efficiency can be improved by increasing the applied potential. Therefore, raising the applied potential can enhance the separation efficiency and decrease the analysis time, both of which are desirable. However, increasing the applied potential can result in very serious Joule heating in the column [12]. This heating and the resulting temperature rise can reduce the separation efficiency due to temperature gradients or lead to failure of the separation if bubbles form. Joule heating can be alleviated by efficient heat dissipation. In practice, very serious Joule heating, corona formation and arcing can occur at voltages above 35 kV. Thus, raising the applied potential can only increase separation efficiency and decrease the analysis time to a point. A capillary with greater surface area will have superior heat dissipation. The heat Q generated in CE is [7],

$$Q=V^2h^2a\lambda c/L^2 \quad (1.5)$$

where h is the height of a rectangular channel, a is the aspect ratio, λ is the molar conductivity of the buffer and c is the buffer concentration. From (1.5), heat generation increases with V^2 or h^2 and scales inversely with L^2; Thus, one way to reduce heat generation is to decrease h through miniaturization of the separation column. With a sufficient reduction in channel dimensions, the applied potential can be increased to enhance the separation efficiency, while the length of the channel can be decreased to shorten the analysis time [7].

1.4 Microchip CE

Advantages of miniaturization of separation systems are reduced sample consumption, faster analysis and higher applied voltages, which can enhance the separation performance as outlined in section 1.3. In recent years, significant interest has arisen in microfluidic devices. More than 25 years ago, the first miniaturized analysis device, a gas chromatographic analyzer fabricated on silicon, was presented [13]. Little additional research was done until 1990, when a miniaturized open-tubular liquid chromatograph on a silicon wafer was fabricated [14]. Simultaneously, the concept of a “miniaturized total chemical analysis system” (μTAS) was proposed by Manz and coworkers [15]. Conceptually, μTAS instrumentation should integrate injection, separation and detection of a sample in a

single miniaturized device. The first successful demonstration of the μTAS concept involved CE microchips [16]. This paper demonstrated that automated, repetitive sample injection and separation on a time scale of seconds were achievable in a miniaturized system. A typical microchip CE (μ-CE) device such as those described by Harrison and Manz [16] consists of a glass substrate with photolithographically patterned and chemically etched channels that are thermally annealed to a glass cover plate having access holes to serve as buffer reservoirs and provide fluidic and electrical contact with the microchannels.

Silicon and glass substrates dominated the early years of microchip fabrication, but a trend toward polymeric substrate materials has developed [17]. In 1997 imprinted poly(methyl methacrylate) (PMMA) substrates were used to fabricate microfluidic devices, which were applied in separating fluorescent analtives [18]. That same year, an integrated μ-CE device was developed in poly(dimethylsiloxane) (PDMS) elastomer to separate fluorescently labeled nucleic acids; the good adhesion of PDMS to other substrates avoided complicated bonding procedures for making devices [19].

Polymer surfaces often need to be modified to ensure optimum biocompatibility [20]. Atom-transfer radical polymerization (ATRP) is a novel technique that can prepare polymers with controlled length in solution [21, 22] or on the surface of the channels of a CE microdevice [20]. For example, ATRP has been used to graft

polyacrylamide onto PDMS [23] to make μ-CE devices for protein separation [24]. ATRP was also applied to graft poly(ethylene glycol) on the surface of PMMA μ-CE devices [20], which allowed fast, reproducible and efficient separations of proteins and peptides.

1.5 Sample Preconcentration

Microchip separation devices have attracted considerable attention due to their rapid analysis times and small sample input requirements. However, since many biological specimens have low concentrations, and small sample volumes are loaded in microchip systems, higher analyte concentrations or more sensitive detectors are typically needed. To decrease the detection limit, laser-induced fluorescence is often used in biological sample analysis. On the other hand, sample preconcentration followed by CE is an alternative approach to enhance the signal intensity from dilute biological samples.

Methods for on-line preconcentration include field-amplified sample stacking (FASS), solid-phase extraction (SPE) and isotachophoretic preconcentration (ITP). FASS uses a gradient in electrolyte conductivity to subject sample ions to nonuniform electric fields. The sample is dissolved in a relatively low conductivity buffer, whose electrical resistance is high in comparison with the rest of the column. Sample ions stack as they exit the high-field, high-velocity region and enter

the low-field, low-velocity segment. A concentration factor of 1,100 was obtained using FASS in a CE chip designed by Jung and coworkers [25]. A microchip for ITP preconcentration coupled with CGE resulted in a 40-fold protein sample enrichment compared to the CGE mode alone [26]. Monolithic porous polymers generated within microchannels in an SPE preconcentration device have been developed, and a concentration factor of 10^3 was achieved [27].

Khandurina et al. [28, 29] demonstrated size-selective structures for DNA concentration prior to CE; channels were connected electrically through small pores in a thin sodium silicate layer. DNA molecules were driven electrokinetically to the sodium silicate membrane but couldn't traverse it, while buffer ions did, such that over time the concentration of the trapped DNA increased ~100-fold. Recently, a protein preconcentration microdevice similar to the DNA systems was constructed, and signal enhancement of ~600-fold was obtained [30]. A microfluidic sample preconcentration system based on electrokinetic trapping at nanopores has been shown to concentrate samples as much as 10^6 - 10^8 fold [31]. Electric field gradient focusing (EFGF) is a technique that uses an electric field gradient and an opposing hydrodynamic flow to enrich and separate proteins. Capillary-based EFGF systems have been demonstrated to concentrate proteins up to 10,000 fold [32].

1.6 Thesis Overview

My research was concerned with sample concentration prior to CE separation. I designed and fabricated two different types of microfluidic sample preconcentrators, a capillary-based setup and an integrated microchip system. The capillary-based preconcentrator is described in Chapter 2. For these devices, fused silica capillaries, metal wire, a polymer membrane and PMMA substrates were used in fabrication, and >1,000-fold concentration factors were obtained. The integrated microdevices are discussed in Chapter 3. Two bonding methods were used to fabricate micromachined devices: polymerization and solvent bonding [33]. In these systems an imprinted channel was enclosed between two PMMA substrates, and protein enrichment factors above 10,000-fold were achieved. Issues with device operation will also be discussed. Finally, conclusions and potential future work are given in Chapter 4. In particular, ATRP surface modification [21, 22] should be a powerful tool to solve fabrication and operation problems.

2. CAPILLARY-BASED PROTEIN PRECONCENTRATION DEVICES

2.1 Introduction

Capillary electrophoresis (CE) is an important separation technique that has been described in section 1.2. CE provides efficient mobility-based separation of biological samples such as peptides, proteins and DNA. Because of the small injection volume and short detection pathlength in CE, it is advantageous to concentrate biological samples prior to separation. Several approaches for sample preconcentration have been described in section 1.5. On-column preconcentration systems connect sample enrichment and CE separation directly on the same platform, such that concentrated proteins can be separated by CE without any manual sample transfer steps.

In this chapter I describe capillary-based protein preconcentration devices made from PMMA substrates, fused silica capillaries and a conductive polymer membrane [33]. When protein is driven electrically toward the membrane, enrichment occurs because the pore size is too small for protein passage. In this system I have achieved 1,000-fold protein sample concentration in 30 minutes.

2.2 Experimental and Fabrication

2.2.1 Materials and sample preparation

Buffer solutions were made using water from a Barnstead EasyPure UV/UF system (Dubuque, IA). Tris buffer (20 mM or 100 mM, pH 8.0) was prepared from Tris HCl and Tris base; the pH was adjusted to 8.0 with HCl. R-phycoerythrin (R-PE; Polysciences, Warrington, PA) and recombinant enhanced green fluorescent protein (GFP; Clontech, Palo Alto, CA) were used after dilution in 20 mM Tris buffer. Standard R-PE solutions (500 ng/mL, 32.0 μg/mL, 62.5 μg/mL, 125 μg/mL, 250 μg/mL, 500 μg/mL and 1 mg/mL) were also prepared in 20 mM Tris buffer.

Fused silica capillaries (150-μm ID) were obtained from Polymicro (Phoenix, AZ). The capillaries were coated dynamically with poly(vinyl alcohol) to control the electroosmotic flow [10]. A 100-μm-diameter Nichrome wire was used to form the microchannel within the membrane. Poly(methyl methacrylate) (PMMA) substrates (Acrylite OP-3) for device fabrication were obtained from Cyro (Rockaway, NJ).

2.2.2 Ion-permeable polymer membrane [33]

Monomers for forming the ion-permeable hydrogel were obtained from Aldrich (Milwaukee, WI). The membrane was a UV-polymerized hydrogel containing 23% methyl methacrylate (MMA), 33% hydroxyethyl methacrylate (HEMA), 20% polyethylene glycol acrylate (PEGA), 3.3% ethylene glycol dimethacrylate (EDMA), 1% 2,2-dimethoxy-2-phenylacetophenone (DMPA), and 20% 100 mM, pH 8.0 Tris

buffer. The mixed components formed a transparent prepolymer solution. In this formulation, MMA provided mechanical strength and rigidity of the membrane, HEMA and PEGA made the membrane hydrophilic, EDMA served as a crosslinker, DMPA was the photoinitiator, and the Tris buffer gave the membrane ionic conductivity.

2.2.3 Instrumentation

Laser-induced fluorescence (LIF) was used to detect the concentrated and separated proteins. Radiation from an air cooled Ar ion laser (488 nm) was directed into an inverted optical microscope (TE300, Nikon, Tokyo, Japan), traversing an excitation filter (D488/10, Chroma, Brattleboro, VT) and being focused by an objective. Fluorescence was collected with this objective, passing through a 505 LD dichroic filter (Chroma) and an E515LPm long-pass filter (Chroma). For point detection of proteins, the laser was passed through a 10X beam expander (Newport, Irvine, CA) prior to focusing the laser light with a 20X 0.45 N.A. objective. Fluorescence was detected by a photomultiplier tube (PMT) (Hamamatsu HC 120-05 Bridgewater, NJ) after spatial filtering with a 200-μm-diameter pinhole. The fluorescence signal from the PMT was filtered and amplified using a SR-560 preamplifier (Stanford Research Systems, Sunnyvale, CA), and the analog output was digitized by a PCI-6035E (National Instruments, Austin, TX) card controlled by LabVIEW (National Instruments) software running on a Dell computer. For

fluorescence imaging, the unexpanded laser was focused on the substrate with a 4X 0.12 N.A. objective. LIF from the device was collected with the same objective and recorded at either a Nikon Coolpix 995 digital camera for color images, or a cooled CCD (Coolsnap HQ, Roper, Tuscon, AZ) for quantitative concentration measurements. A 200 ms exposure time was used for the cooled CCD, and the average intensity in the channel was determined for each CCD image.

2.2.4 Device fabrication

A schematic diagram of the fabrication procedure is given in Figure 2.1. Two 35 x 20 x 1.5 mm PMMA substrates were cut with a CO_2 laser cutter (C-200, Universal Laser Systems, Scottsdale, AZ). The top PMMA substrate included a 10 mm diameter membrane reservoir opening and a channel for aligning the fused silica capillary (see Figure 2.1A). The bottom PMMA substrate also had a straight groove for capillary alignment. Nichrome wire was threaded through two ~3 cm long fused silica capillaries, and the capillaries were placed with their ends about 0.5-1 mm apart in the channel on the bottom PMMA substrate. The upper PMMA plate was set atop the lower piece, and the two PMMA substrates were thermally bonded at 170 ^{o}C for 5 min with 800 psi applied. After bonding, the prepolymer solution was pipetted into the membrane reservoir and polymerized under a UV lamp (Model 5000, Dymax, Torrington, CT) at 320 W for 4 min. Then, the wire was pulled out from the polymer membrane, leaving a 100 μm ID open channel inside the ion-permeable membrane

bridging between the two capillaries (Figure 2.1B-C).

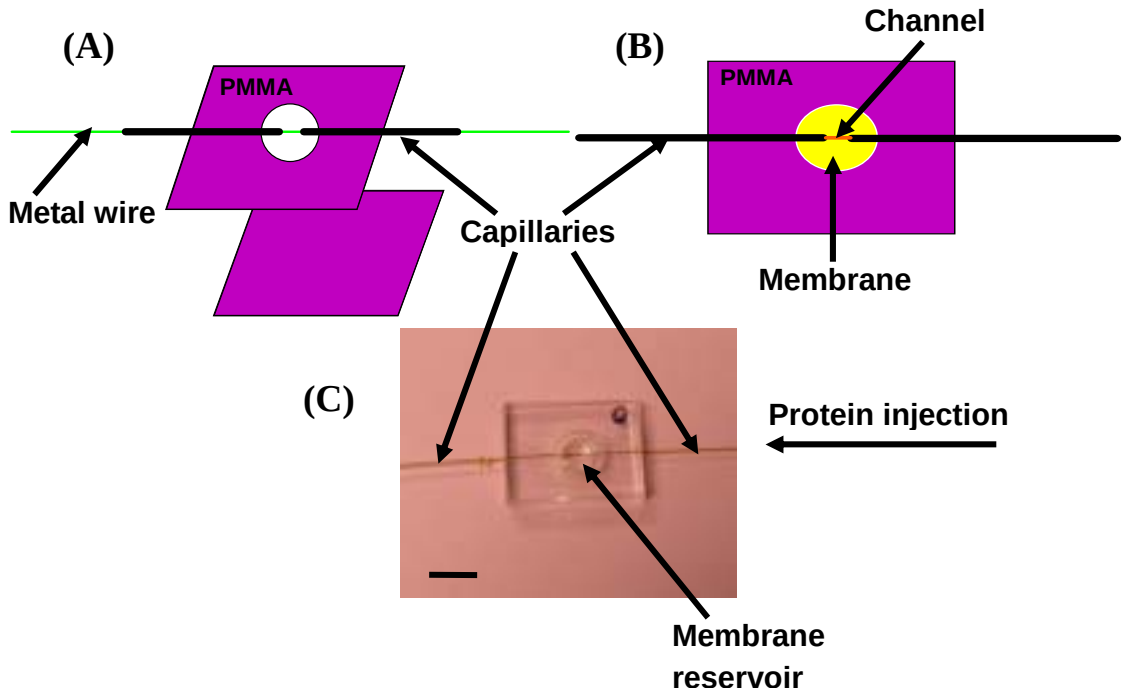

Figure 2.1. Schematics of a capillary-based preconcentration microdevice. (A) Exploded view. (B) Assembled device view. (C) Photograph of device. Additional description is in the text. The scale bar is 1 cm.

2.2.5 Device operation

To focus proteins, one capillary (left, Figure 2.1C) was connected to a plastic tube from a syringe pump through which buffer solution was introduced into the channel, and the end of the other capillary (right, Figure 2.1C) was placed in the sample tube. Buffer solution was added on top of the hydrogel in the membrane reservoir, and platinum electrodes were placed in the sample tube and the membrane reservoir. Protein samples (R-PE or GFP) were loaded into the channel electrokinetically from the right capillary when +500 V were applied to the membrane reservoir and the sample solution was grounded. Because the polymer

membrane was ionically conductive, a current flowed through the channel, and protein accumulated over time in the focusing channel near the membrane since the membrane pore size was too small to allow protein passage.

A calibration curve was made by flowing different concentrations of standard R-PE solutions through the channel using a syringe pump and measuring their LIF signals with a CCD. To study the concentration factor, 500 ng/mL R-PE in 20 mM Tris buffer was continuously loaded electrokinetically toward the membrane for 30 min. The R-PE concentration in the focusing region was determined by comparison with the calibration curve. The average LIF intensity from three replicate images was taken for each standard R-PE solution.

Additional experiments on eluting the focused protein band were also carried out. After protein enrichment, the potentials were altered to apply + 2,000 V at the sample reservoir and ground at the membrane reservoir. Thus, focused protein was eluted from the channel and passed through a transparent window where LIF signal was measured using point detection with the PMT.

2.3 Results and Discussion

Figure 2.2 demonstrates that GFP and R-PE can be enriched successfully in a capillary-based preconcentration device when voltage is applied between the sample reservoir and the membrane. A plot of the R-PE standard concentration versus the

average fluorescence signal was made, which formed a calibration curve (Figure 2.3A). The calibration curve was not linear at higher R-PE concentrations because self-quenching and self-absorbance occurred, which limited the intensity of the fluorescence signal. A 500 ng/mL solution of R-PE was driven electrokinetically toward the membrane for 30 min and enriched; the R-PE concentration was recorded as a function of time to yield the enrichment curve shown in Figure 2.3B. Using the calibration curve and the maximum CCD signal from enriched R-PE (~2,000), the R-PE concentration at the membrane reservoir was found to be ~860 μg/mL with a standard deviation of 90， after 30 min of loading. This corresponds to an enrichment factor of ~1,700 over the initial R-PE solution concentration, in good agreement with the theoretical concentration factor estimated from the enrichment time, mobility of R-PE (3.25×10^{-4} cm^2/Vs) [34], and the ~400-μm-long focusing region (Figure 2.2A).

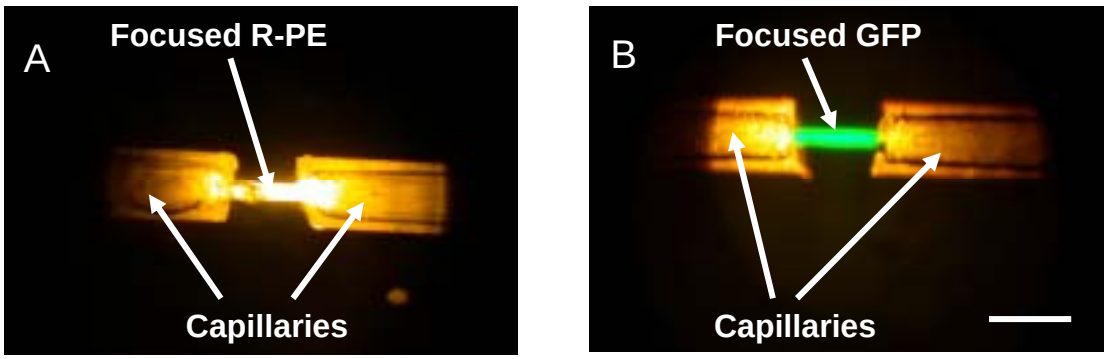

Figure 2.2. Images of focused R-PE (A) and GFP (B) in capillary-based protein preconcentration devices. The scale bar is 500 μm.

In other experiments, the mobilization of a concentrated protein plug was studied. After protein enrichment for 30 min, potentials were switched as indicated in section 2.2.5, and the focused protein was transported from the channel to the detection

window in the capillary. LIF signal was monitored as a function of time with the PMT (see Figure 2.4), and a peak corresponding to the enriched R-PE band was observed at ~170 s.

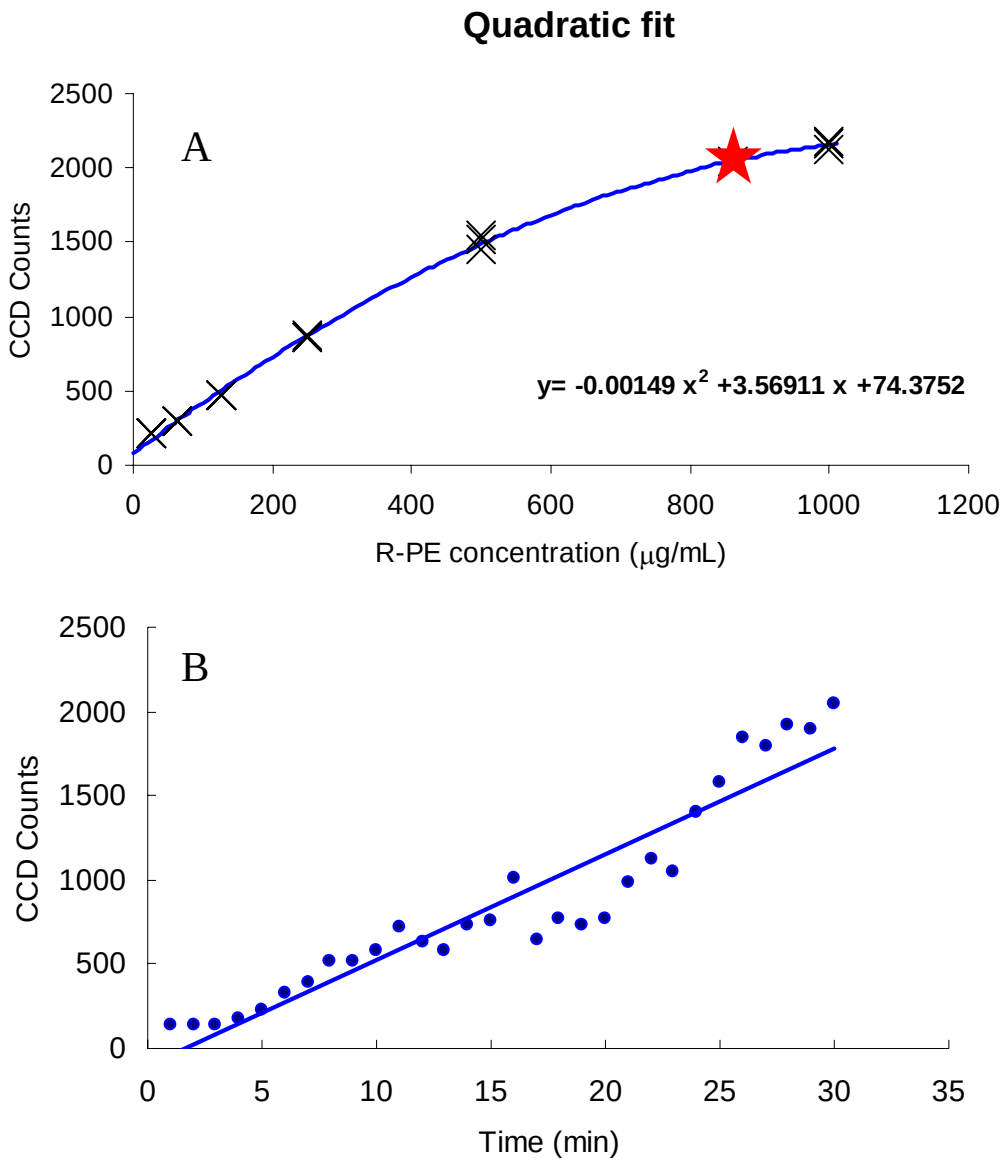

Figure 2.3. R-PE concentration in a capillary device. (A) Calibration curve for CCD signal as a function of standard R-PE concentration. The red star corresponds to the maximum fluorescence signal of concentrated R-PE. Data points for three replicate readings at each concentration are shown. The line is a quadratic fit to the data. (B) Enrichment curve for 500 ng/mL R-PE as a function of time.

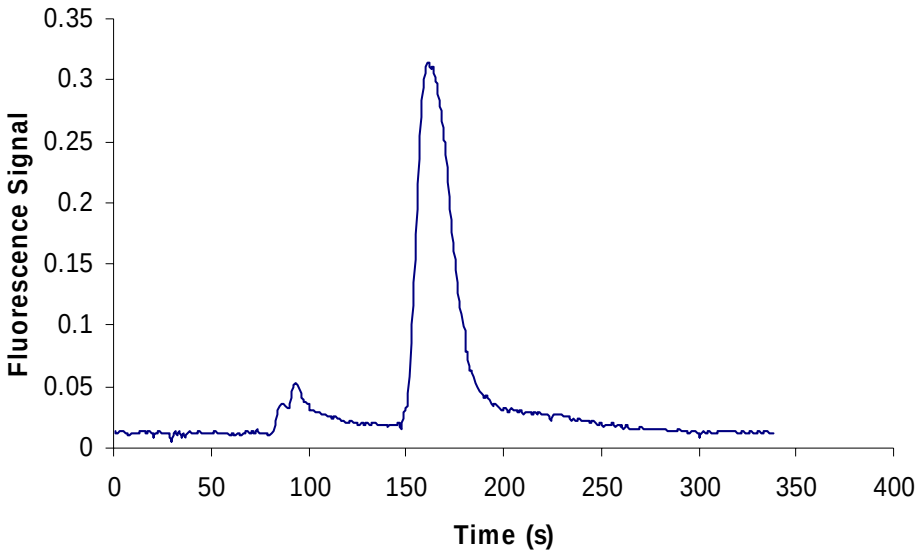

Figure 2.4. Enriched R-PE being eluted from the focusing region. The LIF intensity was recorded as a function of time using a PMT.

One challenge I encountered in these experiments was that after ~10 min of loading, some of the focused protein band began to migrate past the membrane reservoir into a field-free region. This analyte loss is manifested in Figure 2.3B as periodic decreases in the CCD signal. Thus, although a ~1,700-fold enrichment factor was obtained after 30 min of concentration, analyte capture was less than perfect. Importantly, if these sample losses could be eliminated, even higher concentration factors could be achieved. Two possible solutions to this unwanted flow problem were explored: appropriate grounding of both capillaries, and adjusting of reservoir heights to minimize hydrodynamic flow. Neither approach eliminated the focused protein band movement, although reservoir level adjustment was not explored exhaustively. The issue of reservoir levels is simple to address in a planar micromachined platform, which I describe in Chapter 3.

2.4 Conclusions and Future Work

A capillary-based protein preconcentration device was designed and fabricated. PMMA substrates, fused silica capillaries, a metal wire and a polymer membrane were used to construct these systems. Samples were loaded electrokinetically into the capillary and driven toward the membrane, where proteins focused in the channel. After 30 min of injection, a protein concentration factor of nearly 2,000 fold was obtained. Moreover, enriched bands were mobilized from the focusing channel after protein concentration. To fully integrate this preconcentration process with conventional CE, an interface between the preconcentrator and CE system should be developed. Future efforts should also focus on the miniaturization of channel dimensions to provide better heat dissipation, reduce sample consumption, decrease analysis system size, and speed up the concentration and separation process. Thus, Chapter 3 describes the fabrication of integrated, micromachined preconcentrator systems.

3. MEMBRANE-BASED INTEGRATED MICROFLUIDIC PROTEIN PRECONCENTRATION SYSTEMS

3.1 Introduction

Capillary electrophoresis (CE) is a very efficient separation method that can fractionate charged molecules according to their electrophoretic mobilities. Interest in miniaturized CE devices has grown rapidly in recent years due to potential benefits such as low sample consumption, fast analysis, low materials costs and high separation performance. Developing microfluidic sample preconcentration devices is significant because higher-concentration samples are often required in μ-CE systems due to their small injection volumes and short detection pathlengths. Importantly, in the microchip format protein preconcentration can be integrated with CE separation in a single device. In this chapter I describe such a membrane-based integrated polymer microfluidic system that combines sample preconcentration with CE separation. Polymerization and solvent bonding methods were both explored in device fabrication, and an ion-permeable polymer membrane was used as a filter to let small buffer ions pass, but to trap large biological molecules. During optimal device operation, protein samples were concentrated more than 10,000 fold at the membrane. Enriched proteins were also separated in the CE module, and a peptide mixture was injected and separated using these integrated systems.

3.2 Experimental

3.2.1 Materials and sample preparation

Buffer solutions were prepared using water from a Barnstead EasyPure UV/UF system (Dubuque, IA). Tris buffer (20 mM or 100 mM, pH 8.0) was made using Tris HCl and Tris base; the pH was adjusted to 8.0 with HCl. Hydroxypropyl cellulose (HPC) (0.5% w/v) was added to the running buffer to decrease electroosmotic flow (EOF) and analyte adsorption on the surface. R-phycoerythrin (R-PE; Polysciences, Warrington, PA) and recombinant enhanced green fluorescent protein (GFP; Clontech, Palo Alto, CA) were used after dilution in 20 mM Tris buffer. Standard R-PE solutions (40.0 ng/mL, 50.0 ng/mL, 100 ng/mL, 300 ng/mL, 500 ng/mL, 32.0 μg/mL, 62.5 μg/mL, 125 μg/mL, 250 μg/mL, and 500 μg/mL) were also prepared in 20 mM Tris buffer. Peptide standards (Sigma-Aldrich, St. Louis, MO) were labeled fluorescently with fluorescein isothiocyanate (FITC; Molecular Probes, Eugene, OR) in dimethylsulfoxide as described by Kelly et al. [34]. Poly(methyl methacrylate) (PMMA) substrates (Acrylite OP-3, Cyro, Rockaway, NJ) were used to fabricate devices. Monomers used to construct the ion-permeable hydrogel were obtained from Aldrich (Milwaukee, WI), and the same membrane formulation as described in section 2.2.2 was used.

3.2.2 Device fabrication

3.2.2.1 Silicon template

Microchannels were imprinted in PMMA with photolithographically patterned, chemically etched silicon substrates. An 800 nm film of SiO_2 was grown on 4 inch diameter silicon wafers (TTI Silicon, Sunnyvale, CA) at 1110 ^{o}C. AZ 3330 photoresist was spin-coated on the surface of the wafers at 6,000 rpm for 60 s. Next, wafers were baked on a hotplate at 90 ^{o}C for 60 s to remove the remaining solvent. Then, the photoresist was exposed to UV radiation for 14 s through a patterning mask using a PLA-501F (Canon, Tokyo, Japan) contact mask aligner. The glass mask was prepared by Dr. Ryan Kelly. After exposure, the wafers were immersed in AZ 3330 developer solution for 30 s, rinsed using deionized water and dried under a N_2 steam. Next, the wafers were heated on a hotplate at 110 ^{o}C for 5 min to hard bake the photoresist and then etched in 10% buffered HF solution for ~8 min to remove the unprotected silicon dioxide. Finally, the wafers were etched in a 40% KOH solution at 70 ^{o}C for 30-40 min to form the templates.

3.2.2.2 Polymerization bonding

Base substrates and cover plates were cut from a sheet of PMMA using a laser cutter as described in section 2.2.4. The cover plate had one membrane reservoir, one sample reservoir and three buffer reservoirs (see Figure 3.1A). Microchannels were thermally imprinted in the base substrates using a silicon template at 120 ^{o}C for 30

min. A piece of poly(dimethylsiloxane) (PDMS; Sylgard 184, Dow Corning, Midland, MI) was made with four openings that aligned well with the sample reservoir and three buffer reservoirs on the top PMMA substrate. After thorough cleaning, this PDMS slab was placed on the base substrate to seal the imprinted channel (Figure 3.1B). The PDMS/PMMA assembly was put on a hotplate at 70 ^{o}C for 5 min, and liquefied Crème wax (Yaley Enterprises, Redding, CA) was filled into the channels under vacuum (Figure 3.1C). When the assembly was cooled to room temperature, the Crème wax solidified. The PDMS piece was immediately removed from the PMMA substrate, and the cover plate was placed on top. The two pieces of PMMA were clamped together, and Crème wax was added to the buffer and sample reservoirs. Prepolymer solution was added to the membrane reservoir, which also filled the small gap between the two PMMA substrates; the device was then exposed to UV light for 5 min to polymerize the hydrogel. This provided a preconcentration membrane and bonded the two pieces together (Figure 3.1D). After polymerization, the device was heated to 70 ^{o}C, and the liquefied Crème wax was removed from the channels by suction. Finally, hexanes and cyclohexane were flushed through the channels to dissolve any remaining wax, leaving open microchannels that were ready to use (Figure 3.1E). A photograph of a microchip preconcentration device is shown in Figure 3.2.

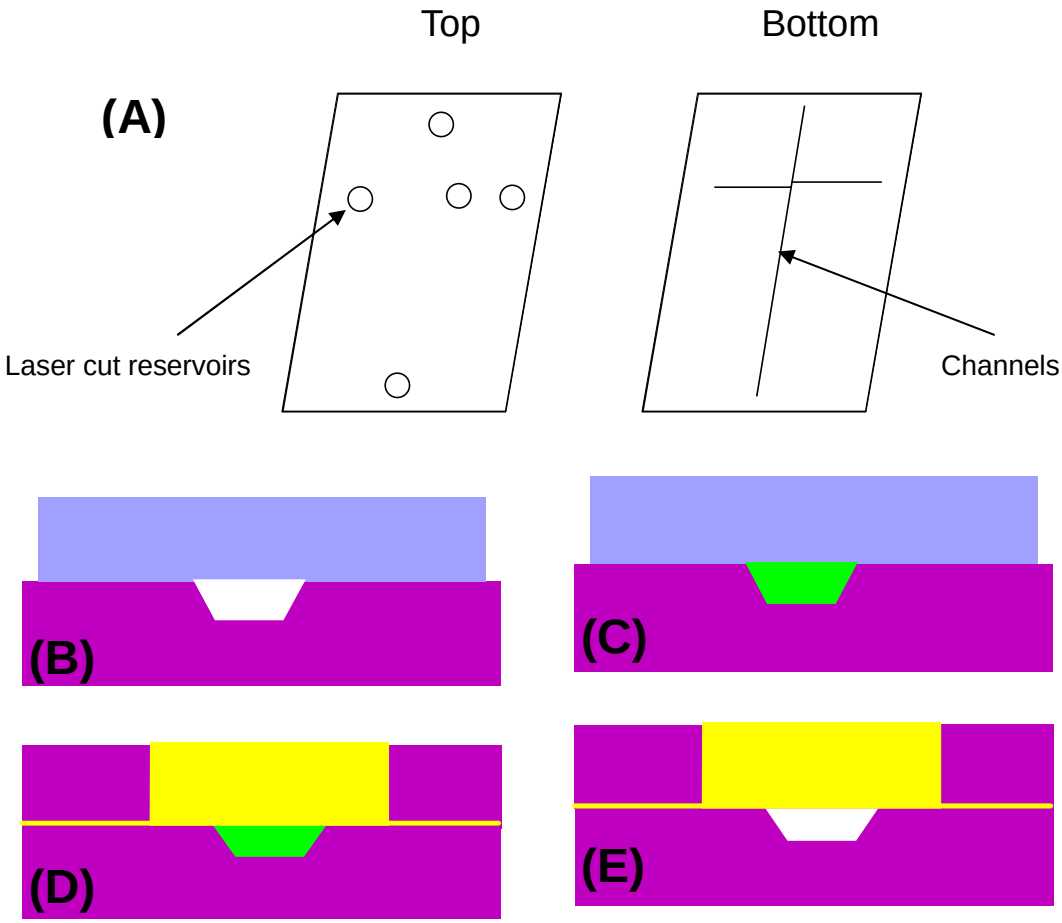

Figure 3.1. Schematics of polymerization bonding device fabrication. (A) Top view of top and bottom substrates. (B) A PDMS piece (blue) is placed on an imprinted PMMA substrate (purple) to form enclosed microchannels. (C) The assembly is heated, and liquid Crème wax (green) is pumped into the microchannels. Then, the device is cooled to solidify the wax, the PDMS is removed and a PMMA substrate with an opening is placed on top. (D) Prepolymer solution is added to the well, and the ion-permeable hydrogel (yellow) is photopolymerized. (E) The wax is melted and removed, leaving an open channel interfaced with the hydrogel membrane.

3.2.2.3 Solvent bonding

I also evaluated device fabrication by solvent bonding, in which an organic solvent (acetonitrile) was used to affix the two PMMA substrates together [34]. This device construction approach is illustrated schematically in Figure 3.3. Crème Wax was used to protect the microchannel as outlined in section 3.2.2.2 (Figure 3.1B-C).

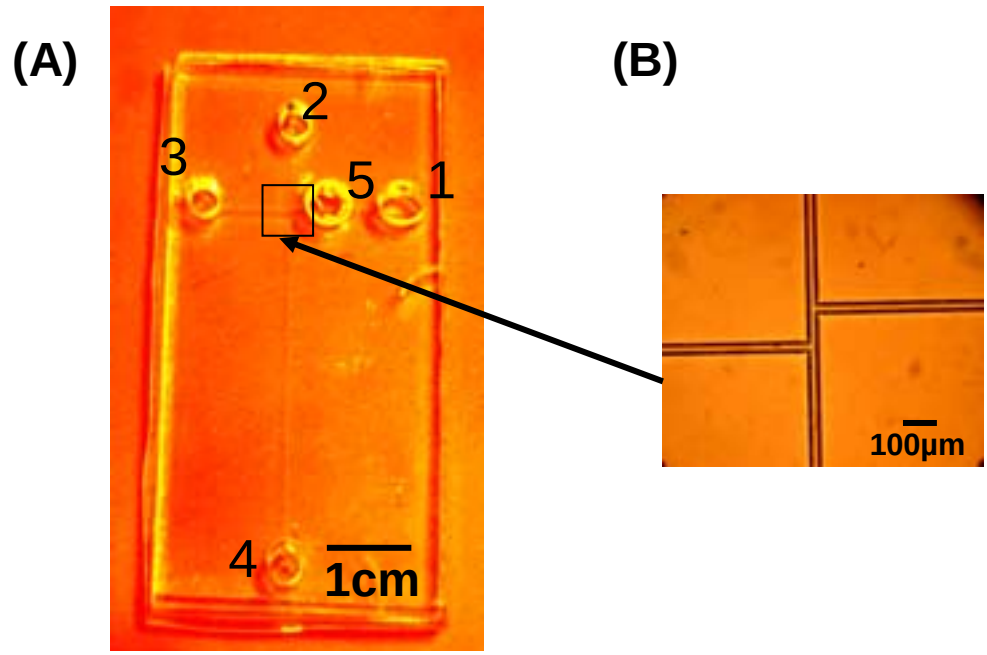

Figure 3.2. Photograph of an integrated microchip device. (A) Reservoir 1 is the sample reservoir, reservoirs 2-4 are buffer reservoirs and 5 is the membrane reservoir. (B) Magnified view of the injection cross region.

Acetonitrile was applied on the wax-protected PMMA microchannel substrate (Figure 3.3A), and immediately thereafter the top PMMA piece was bonded to the bottom substrate using applied pressure for ~2 min (Figure 3.3B). Ionically conductive membrane polymerization and Crème wax removal (Figure 3.3C-D) were carried out as described in section 3.2.2.2.

3.2.3 Instrumentation

Laser-induced fluorescence detection was carried out as described in section 2.2.3.

3.2.4 Device operation

The microchip devices were filled with 20 mM Tris buffer containing 0.5% HPC,

and protein was loaded into the sample reservoir. Electrodes were inserted into each

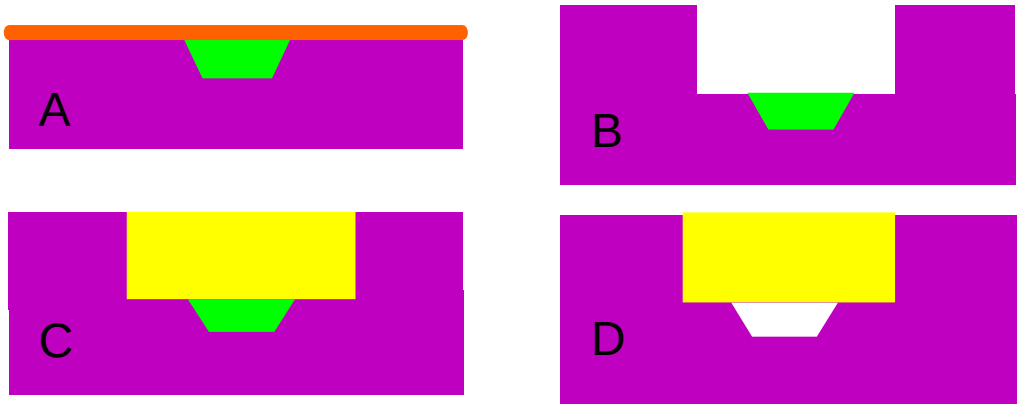

Figure 3.3. Schematic diagram of solvent-bonded device fabrication. (A) Acetontrile (orange) is applied on a substrate (purple) with a Crème wax-protected PMMA microchannel (green). (B) A PMMA piece with an opening is bonded on top of the microchannel substrate. (C) Prepolymer solution is introduced into the well, and the ion-permeable hydrogel (yellow) is photopolymerized. (D) The Crème wax is melted and removed from the channel.

of the five reservoirs. For preconcentration experiments, +500 V were applied to the membrane reservoir (5), and all other reservoirs were grounded. Negatively charged proteins (5 μg/mL R-PE and GFP) were driven electrokinetically through the microchannel to the membrane, where they were concentrated. In some instances, the focused proteins were transferred to the injection region by removing the membrane reservoir electrode, applying +500 V to reservoir 3 and grounding all other reservoirs. A small plug of enriched protein was injected for CE analysis by applying +800 V to reservoirs 1 and 3, +2,000 V to reservoir 4 and grounding reservoir 2 (see Figure 3.2 for reservoir numbering). In this voltage configuration, the injected proteins were separated by CE; laser-induced fluorescence was detected by a color digital camera. In addition, I evaluated whether or not these devices could enrich peptides (15 μM

Ang I and Ang II). This peptide mixture was also separated in these devices without a preconcentration step by using the injection and separation voltages described above for proteins. Laser-induced fluorescence in peptide separations was detected using the photomultiplier tube system.

3.2.5 Calibration curve

A calibration curve was made by flowing different concentrations of standard R-PE solutions through the microchannel in polymerization-bonded microdevices. A cooled CCD was used to record the average fluorescence signal of each flowing standard R-PE solution.

3.3 Results and Discussion

Integrated protein preconcentration microchips were constructed using two different enclosure methods: polymerization and solvent bonding. Both approaches were successful in fabricating microdevices, and each technique for making these microchips had advantages and disadvantages, as discussed below. To determine the extent of protein enrichment at the membrane, I made a calibration curve plotting the mean CCD fluorescence signal vs. the concentration of R-PE standard solution flowing through the microchip (Figure 3.4). Linear regression of the standard R-PE solution data yielded a slope of 1.92 with a standard deviation of 0.05, an intercept of -8 with a standard deviation of 13 and an R^2 value of 0.9978.

3.3.1 Polymerization-bonded microchips

In polymerization-bonded devices, the CCD signal from R-PE samples over 50 ng/mL exceeded the calibration curve range after 30 min of concentration, so their enrichment factor could not be quantified. With 100 ng/mL R-PE and a 10 min focusing time, a 1,000-fold increase in sample concentration was obtained. With longer sample enrichment times, R-PE continued to concentrate such that the CCD signal exceeded the range of the calibration curve. When 40 ng/mL R-PE was transported electrokinetically to accumulate at the membrane for 40 min, an average CCD signal of 850 was obtained. This detector output corresponds to a concentration of 450 µg/mL (Figure 3.4), a >10,000-fold enrichment factor over the initial concentration.

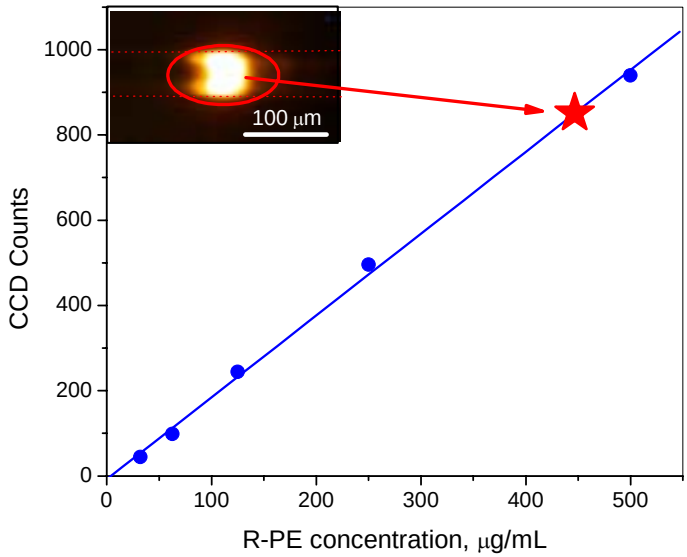

Figure 3.4. Calibration curve for CCD signal as a function of R-PE concentration in flowing standard solutions. R-PE with the concentration of 40 ng/mL in 20 mM Tris was concentrated at the membrane reservoir for 40 min. (Inset) CCD image of 40 ng/mL R-PE enriched at the membrane after 40 min; the mean signal from this image

corresponds to the red star on the calibration curve.

A key advantage of this integrated system is its ability to both concentrate and separate samples on the same platform without manual transfer steps. The successful results of one such experiment are shown in Figure 3.5. A mixture of 5 μg/mL R-PE and GFP was loaded electrokinetically from the sample reservoir for 30 minutes as described in section 3.2.4, resulting in a narrow, concentrated protein plug in the injection channel at the membrane (Figure 3.5A). This concentrated protein mixture was transferred to the double T injection region for 30 seconds as described in section 3.2.4, moving the enriched analytes to the injector (Figure 3.5B). Finally, the enriched protein mixture was separated electrophoretically when voltage was applied along the separation channel (Figure 3.5C), demonstrating the successful coupling of on-chip preconcentration with microchip CE.

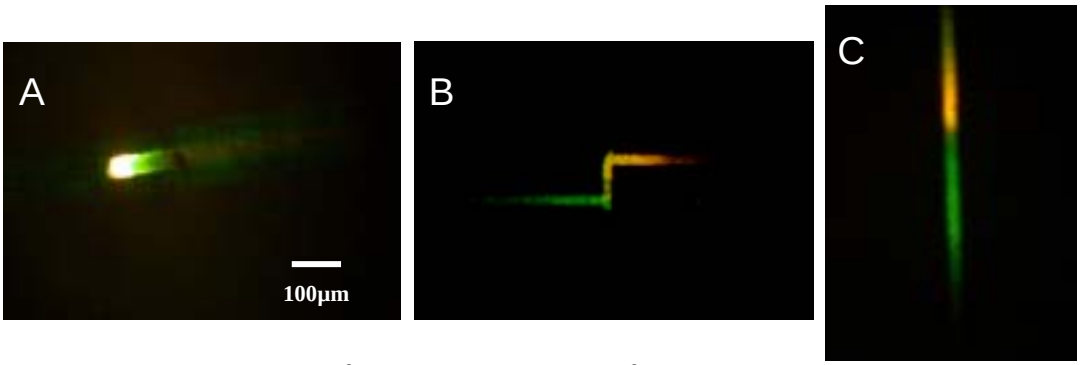

Figure 3.5. Digital camera fluorescence images of the preconcentration, injection and CE separation of R-PE and GFP. (A) R-PE and GFP at the membrane region after enrichment for 30 min. (B) The concentrated band in (A) is electrokinetically driven to the injection region. (C) Image of the separation column 15 mm from the injection region 1 min after starting CE; R-PE (top band, yellow) and GFP (lower band, green) are already resolved.

In addition, I tried to concentrate FITC-labeled Ang I and Ang II peptides at the membrane reservoir. Even for very short (~5 s) enrichment times, significant

amounts of peptide penetrated the membrane and disappeared from the channel. I hypothesize that the pore size of the membrane (optimized for proteins) was too large to retain peptides effectively. To concentrate peptides in these integrated devices, the formulation of the membrane monomer solution should be modified to decrease the pore size to trap peptide molecules better.

To further assess the separation performance of the CE component of the integrated preconcentration microchips, FITC-labeled Ang I and Ang II were injected and separated directly, without an enrichment step. Figure 3.6 shows a μ-CE separation of Ang I and Ang II in under 50 seconds using a polymerization-bonded device. The two peaks differ in migration time by 7.6 seconds, and their resolution was 1.6. The number of theoretical plates for Ang II is 4,300 and for Ang I is 3,500 (2.5 cm length and 2,000 V applied). The separation efficiencies are lower than what has been reported in conventional CE with longer capillaries and higher applied potentials [35], but the microchip analysis time was ~10 times faster.

One challenge with polymerization-bonded microchips was poor reproducibility of injection and separation between devices. For example, sometimes a 30 second injection was enough, but other times more than 5 min were needed. I believe that the reproducibility issues were due to surface effects in these devices. Because three sides of the channel walls were PMMA and the other surface was the polymer membrane, the surface charge was not uniform in the channel. These surface charge

effects can cause flow inhomogeneities, which can hamper device reproducibility.

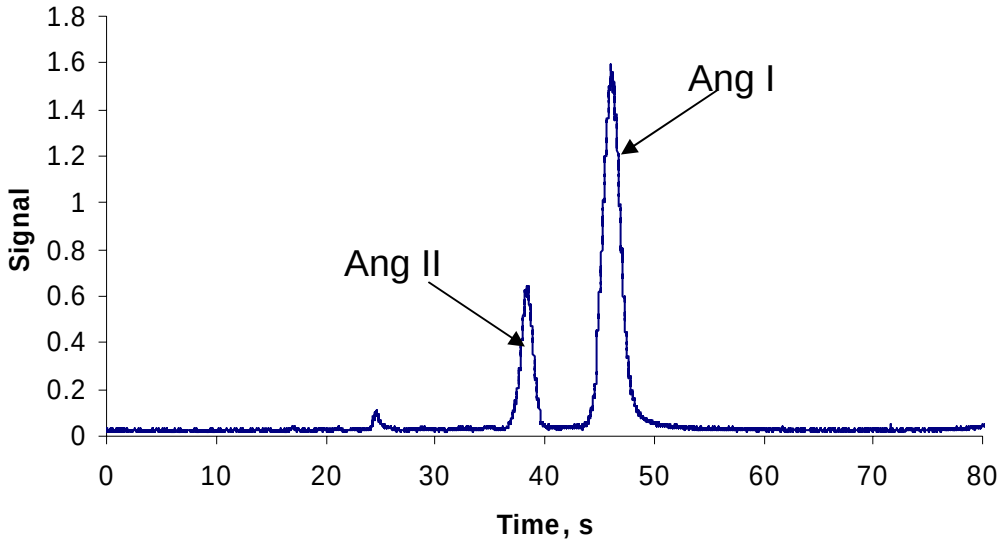

Figure 3.6. Separation of FITC-labeled Ang I and Ang II peptides by μ-CE in a polymerization-bonded microdevice. Peptide concentrations were 15 μM, and the buffer was 20 mM Tris, with 0.5% (w/v) HPC added to suppress electroosmotic flow. The separation potential was 2,000 V.

In addition, sample adsorption for both proteins and peptides was observed in these channels. This led to loss of analyte and altered electroosmotic flow, either of which could impair device performance. These problems persisted, but were not quite as severe when HPC, a surface passivating agent, was added to the running buffer. These surface issues should be eliminated if one covalently modifies the channel walls, something that is straightforward using a recently reported PMMA surface modification method that grafts a layer of poly(ethylene glycol) on the channel [20].

3.3.2 Solvent-bonded devices

For solvent-bonded microchips, the entire channel surface was PMMA, so non-uniform EOF was not a problem in separation, as it was for polymerization-bonded devices. One challenge associated with the membrane formulation used in solvent-bonded microchips was that the hydrogel shrank somewhat during polymerization, leaving a small gap between the membrane and the PMMA substrate. When a potential was applied between the membrane and sample reservoirs, protein was concentrated against the membrane just as in polymerization-bonded systems. However, the gap between the membrane and PMMA led to some protein loss from the channel, as shown in Figure 3.7. Because of this issue, I did not determine the concentration factor in solvent-bonded devices.

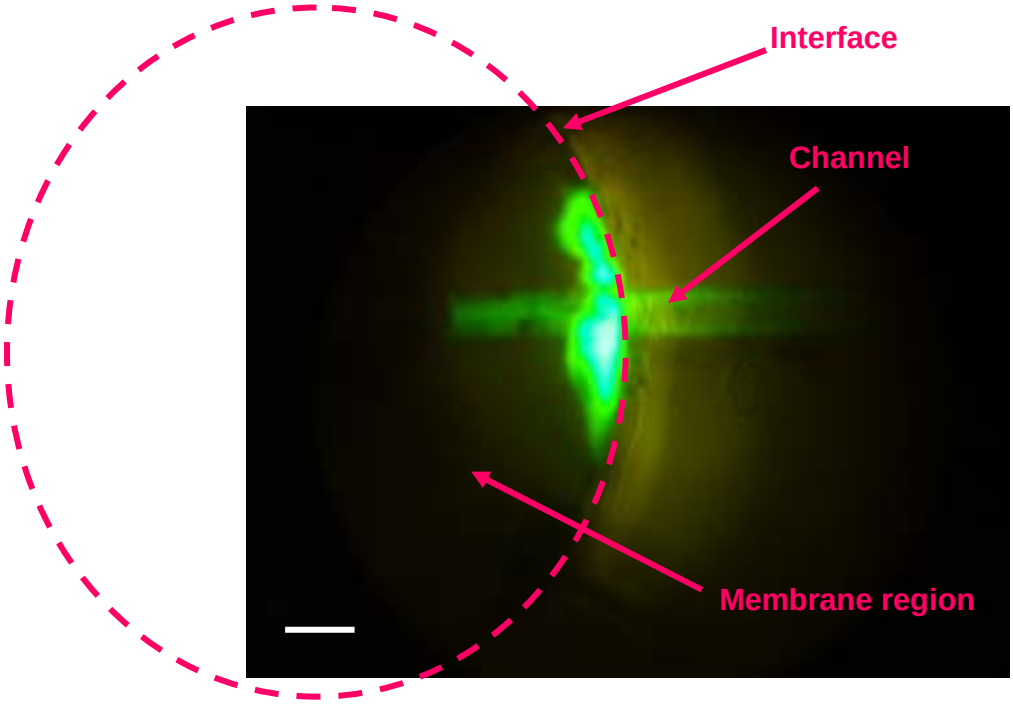

Figure 3.7. Fluorescence image showing GFP leaking into the gap between the membrane and PMMA in a solvent-bonded device. The scale bar is 100 μm.

3.4 Conclusions

Integrated preconcentration / CE microchips were developed using two different fabrication methods involving polymerization and solvent bonding. For solvent-bonded devices, the substrates were sealed well, but small gaps at the membrane-PMMA interface hampered quantitation of the enrichment factor. For polymerization-bonded devices, the hydrogel membrane served both as a glue to affix the PMMA substrates together for channel enclosure and to form a size-selective barrier for analyte enrichment. Peptide mixtures of Ang I and Ang II were separated using polymerization-bonded integrated microchips. Moreover, when an electrical potential was applied along the channel, more than 10,000-fold protein enrichment was obtained. Finally, a protein mixture containing R-PE and GFP was concentrated, injected and separated in these integrated devices.

4. CONCLUSIONS AND FUTURE WORK

4.1 Conclusions

I have designed, fabricated and operated two different types of microfluidic protein preconcentration devices. Capillary-based protein enrichment systems were fabricated using PMMA substrates, fused silica capillaries and an ion-permeable membrane. When 500 V were applied between a sample reservoir and the membrane for 30 min, proteins were enriched almost 2,000-fold in the channel. I have also evaluated membrane-based microchip devices that integrate protein preconcentration and separation. Microchannels were imprinted using silicon templates, and an ionically conductive membrane was interfaced with the channel. Two methods were explored to enclose these devices: polymerization and solvent bonding. Device yield issues with solvent-bonded substrates led to a greater focus on polymerization bonding. For polymerization-bonded devices, prepolymer was applied between the PMMA substrates and in the membrane reservoir so bonding and membrane polymerization occurred simultaneously during UV exposure. When 500 V were applied between the sample and membrane reservoir for 40 min, proteins were concentrated by a factor of 10,000. In addition, proteins concentrated in this manner were separated in these integrated microchip CE systems. Peptide concentration and separation were also evaluated using polymerization-bonded microchips.

4.2 Future Work

A number of potential improvements to this work could be implemented in future studies. For example, an interface connecting the preconcentrator with CE separation should be developed for capillary-based preconcentration systems. Some device performance issues for integrated microchips should also be addressed in the future. Challenges associated with protein adsorption and irreproducible EOF in polymerization-bonded devices, and the issue of membrane detachment from the PMMA in solvent-bonded systems could both be addressed readily through polymer surface derivatization. Atom transfer radical polymerization (ATRP) has previously been shown as an effective tool for polymer surface modification for grafting an inert layer to avoid sample adsorption [21, 24]. In a similar fashion, ATRP surface modification could be used to attach molecules with free double bonds to the membrane reservoir surface to covalently anchor the polymer hydrogel and avoid the formation of voids at the membrane-PMMA interface.

Here, I outline a procedure that could be used for grafting unsaturated moieties to PMMA to enhance membrane-to-PMMA adhesion. First, an oxygen plasma will oxidize the PMMA surface, creating hydroxyl or carboxyl groups on the surface (Figure 4.1A). Next, 2-bromoisobutyryl bromide initiator will be immobilized on the activated surface (Figure 4.1B). In the third step, hydroxyethyl methacrylate (HEMA) will be grafted on the PMMA surface, resulting in an increased number of free

hydroxyl groups relative to the oxidation step (Figure 4.1C). This hydrophilic surface should also resist analyte adsorption better than native PMMA. Solvent bonding approaches described in section 3.2.2.3 will be used to enclose channels in modified PMMA substrates. Then, 0.4% solution of 3-methacryloxypropyltrimethoxysilane will be reacted with the HEMA hydroxyl groups on the membrane reservoir surface, leaving free double bonds (Figure 4.1D). Finally, the monomer solution will be placed in the membrane reservoir and UV polymerized to form a hydrogel that will be attached covalently to the activated double bonds on the membrane reservoir surface. This covalent instead of physical attachment between PMMA and the hydrogel should solve the membrane detachment issue.

The fabrication methods developed in my thesis can also be used in the construction of microfluidic devices from other materials. For example, solvent bonding could be applied in fabricating microfluidic devices from polycarbonate or poly(ethylene terephthalate). Finally, polymerization bonding could be explored in making microchips from materials that cannot be affixed together by thermal or solvent bonding methods. In summary, this work describes general and useful microdevice fabrication techniques that have a promising future in the microchip field.

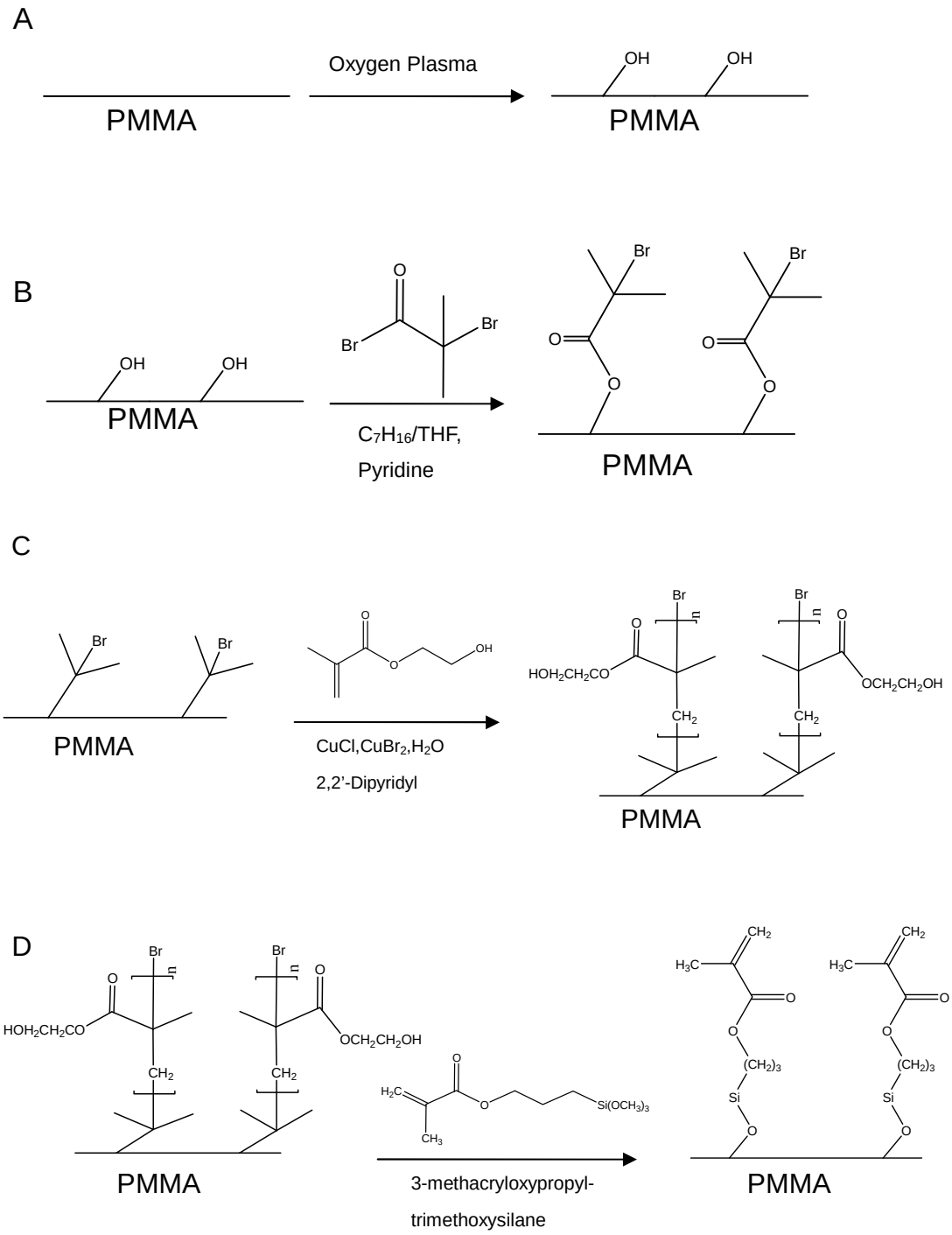

Figure 4.1. Reaction scheme for attaching a hydrogel membrane to the PMMA surface. (A) Oxygen plasma activation of native PMMA. (B) Immobilization of initiator. (C) Grafting of HEMA on the PMMA surface. (D) Reaction of a silane with HEMA to form double bonds on the PMMA surface.

REFERENCES

1. Chen, J.B.; Balgley, B.M.; DeVoe, D.L.; Lee, C.S. Capillary Isoelectric Focusing-Based Multidimensional Concentration/Separation Platform for Proteome Analysis. *Anal. Chem*. **75**, 3145-3152 (2003).
2. Morris, D.L.; Sutton, J.N.; Harper, R.G.; Timperman, A.T. Reversed-Phase HPLC Separation of Human Serum Employing a Novel Saw-Tooth Gradient: Toward Multidimensional Proteome Analysis. *J. Proteome Res.* **3**, 1149-1154 (2004).
3. Zhao, Y.; Desiderio, M.D.; Fang, B.; Beranova-Giorgianni, S. Toward a Global Analysis of the Human Pituitary Proteome by Multiple Gel-Based Technology. *Anal. Chem.* **77,** 5324-5331 (2005).
4. Wu, H.; Bruley, D.F. Homologous Human Blood Protein Separation Using Immobilized Metal Affinity Chromatography: Protein C Separation from Prothrombin with Application to the Separation of Factor IX and Prothrombin. *Biotechnol. Prog.* **15**, 928-931 (1999).
5. Mikkers, F.E.P.; Verheggen, Th.P.E.M. High-Performance Zone Electrophoresis. *J. Chromatogr.* **169,** 11-20 (1979).
6. Jorgenson, J.; Lukacs, K. Free-zone Electrophoresis in Glass Capillaries. *Clin. Chem.* **27**, 1551-1553 (1981).
7. Eijkel, A.M. Miniaturization and Chip Technology. What Can We Expect? *Pure Appl. Chem.* **73,** 1555-1561 (2001).
8. Hayes, M.A.; Kheterpal, I.; Ewing, A.G.. Effects of Buffer pH on Electroosmotic Flow Control by an Applied Radial Voltage for Capillary Zone Electrophoresis. *Anal*. *Chem***. 65,** 27-31 (1999).
9. Krylov, S.N.; Dovichi, N.J. Capillary Electrophoresis for the Analysis of Biopolymers. *Anal. Chem.* **72**, 111-128 (2000).
10. Gllges, M.; Kleemiss, M.H.; Schomburg, H. Capillary Zone Electrophoresis Separations of Basic and Acidic Proteins Using Poly(vinyl alcohol) Coatings in Fused Silica Capillaries. *Anal. Chem.* **66,** 2038-2046 (1994).
11. Gamble, T.N.; Ramachandran, C.; Bateman, K.P. Phosphopeptide Isomer Separation Using Capillary Zone Electrophoresis for the Study of Protein Kinases and Phosphatases. *Anal. Chem*. **71**, 3469-3476 (1999).
12. Xuan, X.C.; Li, D. Joule Heating Effects on Peak Broadening in Capillary Zone Electrophoresis. *J. Micromech. Microeng.* **14,** 1171-1180 (2004).
13. Terry, S. C.; Jerman, J. H.; Angell, J. B. A Gas Chromatographic Air Analyzer Fabricated on a Silicon Wafer. *IEEE Trans*. *Electon Devices,* **26**, 1880 (1979).
14. Manz, A.; Miyahara, Y.; Miura, J.; Watanabe, H.; Miyagi, H.; Sato, K. Design of an Open-Tubular Column Liquid Chromatography Using Silicon Chip Technology. *Sens. Actuators,* **B1**, 249-255 (1990).
15. Manz, A.; Graber, N.; Widmer, H.M. Miniaturized Total Chemical Analysis Systems: A Novel Concept for Chemical Sensing. *Sens. Actuators,* **B1,** 244-248

(1990).
16. Manz, A.; Harrison, D.J.; Verpoorte, E.M.G.; Fettinger, J.C.; Paulus, A.; Lüdi, H.; Widmer, H.M. Planar Chips Technology for Miniaturization and Integration of Separation Techniques into Monitoring Systems: Capillary Electrophoresis on a Chip. *J. Chromatogr.* **593,** 253-258 (1992).
17. Becker, H.; Gartner, C. Polymer Microfabrication Methods for Microfluidic Analytical Applications. *Electrophoresis*, **21**, 12-26 (2000).
18. Martynova, L.; Gaitan, M.; Kramer, G.W.; Christensen, R.G. Fabrication of Plastic Microfluid Channels by Imprinting Methods. *Anal. Chem*. **69**, 4783-4789 (1997).
19. Effenhauser, C.S.; Bruin, G.J.M.; Paulus, A.; Ehrat, M. Integrated Capillary Electrophoresis on Flexible Silicone Microdevices: Analysis of DNA Restriction Fragments and Detection of Single DNA Molecules on Microchips. *Anal. Chem*. **69,** 3451-3457 (1997).
20. Liu, J.K.; Pan, T.; Woolley, A.T.; Lee, M.L. Surface-Modified Poly(methyl methacrylate) Capillary Electrophoresis Microchips for Protein and Peptide Analysis. *Anal. Chem*. **76,** 6948-6955 (2004).
21. Kato, M.; Kamigaito, M.; Sawamoto, M.; Higashimura, T. *Macromolecules,* **28**, 1721-1723 (1995).
22. Wang, J.-S.; Matyjaszewski, K. Controlled/"Living" Radical Polymerization. Atom Transfer Radical Polymerization in the Presence of Transition-Metal Complexes *J. Am. Chem. Soc.* **117,** 5614-5615 (1995).
23. Xiao, D.; Zhang, H.; Wirth, M. Chemical Modification of the Surface of Poly(dimethylsiloxane) by Atom-Transfer Radical Polymerization of Acrylamide. *Langmuir,* **18,** 9971-9976 (2002).
24. Xiao, D.; Le, T.V.; Wirth, M.J. Surface Modification of the Channels of Poly(dimethylsiloxane) Microfluidic Chips with Polyacrylamide for Fast Electrophoretic Separations of Proteins. *Anal. Chem*. **76**, 2055-2061 (2004).
25. Jung, B.; Bharadwaj, R.; Santiago, J.G. Thousandfold Signal Increase Using Field-Amplified Sample Stacking for On-Chip Electrophoresis. *Electrophoresis,* **24,** 3476 (2003).
26. Huang, H.Q.; Dai, Z.P.; Lin, B.C. On-Line Isotachophoretic Preconcentration and Gel Electrophoretic Separation of Sodium Dodecyl Sulfate-Proteins on a Microchip. *Electrophoresis,* **26**, 2254-2260 (2005).
27. Yu, C.; Davey, M.H.; Svec, F.; Frechet, J.M.J. Monolithic Porous Polymer for On-Chip Solid-Phase Extraction and Preconcentration Prepared by Photoinitiated in Situ Polymerization within a Microfluidic Device. *Anal. Chem*. **73**, 5088-5096 (2001).
28. Khandurina, J.; Jacobson, S.C.; Waters, L.C.; Foote, R.S.; Ramsey, J.M. Microfabricated Porous Membrane Structure for Sample Concentration and Electrophoretic Analysis. *Anal. Chem.* **71**, 1815-1819 (1999).

39. Khandurina, J.; McKnight, T.E.; Jacobson, S.C.; Waters, L.C.; Foote, R.S.; Ramsey, J.M. Integrated System for Rapid PCR-Based DNA Analysis in Microfluidic Devices. *Anal. Chem*. **72**, 2995-3000 (2000).
30. Foote, R.S.; Khandurina, J.; Jacobson, S.C.; Ramsey, J.M. Preconcentration of Proteins on Microfluidic Devices Using Porous Silica Membranes. *Anal. Chem.* **77**, 57-63 (2005).
31. Wang, Y.-C.; Stevens, A.L.; Han, J. Million-fold Preconcentration of Proteins and Peptides by Nanofluidic Filter. *Anal. Chem.* **77**, 4293-4299 (2005).
32. Humble, P.H.; Kelly, R.T.; Woolley, A.T.; Tolley, H.D.; Lee, M.L. Electric Field Gradient Focusing of Proteins Based on Shaped Ionically Conductive Acrylic Polymer. *Anal. Chem.* **76**, 5641-5648 (2004).
33. Kelly, R.T.; Pan, T.; Woolley, A.T. Phase-Changing Sacrificial Materials for Solvent Bonding of High-Performance Polymeric Capillary Electrophoresis Microchips. *Anal*. *Chem*. **77**, 3536-3541 (2005).
34. Warnick, K.F.; Francom, S.J.; Humble, P.H.; Kelly, R.T.; Woolley, A.T.; Lee, M.L.; Tolley, H.D. Field Gradient Electrophoresis. *Electrophoresis*. **26**, 405-414 (2005)
35. Lacher, N.A.; Garrison, K.E.; Lunte, S.M. Separation and Detection of Angiotensin Peptides by Cu(II) Complexation and Capillary Electrophoresis with UV and Electrochemical Detection. *Electrophoresis*. **23**, 1577-1584 (2002).